TDP-43 was first isolated as a transcriptional inactivator binding to the TAR DNA element of the HIV-1 virus.[18] It appears to belong to the group of 2 RNA-binding domain (RBD)-Gly RNA-binding proteins, which include the heterogeneous nuclear ribonucleoprotein (hnRNP) family and factors involved in RNA splicing and transport.[19] Subsequent studies reported that TDP-43 functions to inhibit expression of mouse spermatid-specific SP-10 gene and of cyclin-dependent kinase 6, to regulate alternative splicing of exon 9 of cystic fibrosis transmembrane conductase regulator (*CFTR*), exon 3 of apolipoprotein A-II (*Apo AII*), and exon 7 of survival of motor neuron 2 (*SMN2*), and to stabilize human low molecular weight neurofilament (hNFL) mRNA.[20-26] The splicing inhibitory activity requires the C-terminal region of TDP-43 by interaction with other hnRNP members.[27] Furthermore, more recent studies suggest that TDP-43 may be involved in other cellular processes such as microRNA biogenesis, apoptosis, and cell division.[28]

Ubiquitin- and TDP-43-positive pathological inclusions found in FTLD-TDP include neuronal cytoplasmic inclusions (NCIs), dystrophic neurites (DNs), neuronal intranuclear inclusions (NIIs), and glial cytoplasmic inclusions (GCIs).[1,2,29-31] Based on morphological aspects, TDP-43 proteinopathies have been classified into four subtypes.[32] Type 1 is characterized by DNs with few NCIs and no NIIs, Type 2 has numerous NCIs with few DNs and no NIIs, Type 3 has numerous NCIs and DNs and an occasional NIIs and Type 4 has numerous NIIs and DNs with few NCIs. Type 4 is specific for familial FTLD-TDP with mutations of VCP gene. The strong relationship between other subtypes of TDP-43 pathology and clinical phenotype is indicated. Type 1 is associated with semantic dementia, Type 2 with FTLD with motor neuron disease (MND) or clinical signs of MND, and Type 3 with progressive non-fluent aphasia.[29,33,34]

In ALS, motoneuronal skein-like inclusions immunopositive for ubiquitin had been regarded as major pathological hallmarks. Recent detailed immunohistochemical studies have clarified the wide distribution of neuronal and glial TDP-43 pathology in multiple areas of the central nervous systems, including the nigro-striatal system, the neocortical and allocortical areas, and the cerebellum.[35,36] These findings suggest that ALS does not selectively affect only the motor system, but rather is a multisystem neurodegenerative TDP-43 proteinopathy affecting both neurons and glial cells.[35,36]

Biochemical analyses of the detergent-insoluble fraction extracted from brains of patients afflicted with FTLD-TDP and ALS show that TDP-43 accumulated in these pathological structures is phosphorylated and cleaved.[1,2]

In the present review, we will focus on the histological and biochemical abnormality of TDP-43 accumulated in ALS, FTLD-TDP and other neurodegenerative disorders, and on the establishment and analyses of cellular models for intracellular aggregates of TDP-43. Using antibodies specific for phosphorylated TDP-43 (pTDP-43), we identified several phosphorylation sites in the C-terminal region of the TDP-43 that accumulates in FTLD-TDP and ALS brains.[37] Furthermore, we found a close relationship between the pathological subtypes of FTLD-TDP and ALS and the immunoblot pattern of phosphorylated C-terminal fragments of TDP-43, suggesting that proteolytic processing may be crucial in the pathological process of these diseases.[37] By transfecting deletion mutants lacking nuclear localization signal or C-terminal fragments of TDP-43, we succeeded in establishing the cellular models of TDP-43 proteinopathy. By analyzing them, we found the pathogenic effect of mutations of TDP-43 gene identified in ALS cases, and the potential therapeutic agents that inhibit the aggregate formation of TDP-43.

## IMMUNOHISTOCHEMICAL AND BIOCHEMICAL ANALYSIS FOR PTDP-43 IN ALS AND FTLD-TDP

In order to identify the critical phosphorylation sites of TDP-43, we raised antibodies against 39 different synthetic phosphopeptides, representing 36 out of 63 candidate phosphorylation sites.[37] Of the generated antibodies, pS379, pS403/404, pS409, pS410 and pS409/410 stained the inclusions in immunohistochemistry, and abnormal TDP-43 species on immunoblot, in FTLD-TDP and ALS cases. Since the immunoreactivity of pS409/410 was particularly robust in both immunohistochemistry and immunoblotting, we later produced a monoclonal antibody directed against phosphoserines 409 and 410 in human TDP-43.[38] The results suggest that at least five sites on TDP-43 are phosphorylated in subjects with FTLD-TDP and ALS, and that abnormal phosphorylation takes place mainly near the carboxyl (C)-terminal region of TDP-43.

In immunohistochemistry, in contrast to the commercially obtained phosphorylation-independent anti-TDP-43 antibody, which labels both abnormal structures and normal nuclei (Fig. 1A), pTDP-43-specific antibodies recognized only abnormal structures, including NCIs (Fig. 1B), NIIs (Fig. 1B, inset), DNs (Fig. 1C), round inclusions (Fig. 1D), skein-like inclusions (Fig. 1E), and GCIs (Fig. 1F). In double immunofluorescence staining for pTDP-43 (Fig. 1G, red) and a complement protein, C4d (Fig. 1H, green), pTDP-43-positive inclusions were often found in C4d-positive oligodendrocytes (Fig. 1I), indicating that most GCIs are oligodendrocytic in origin. In the frontal cortex of the ALS case with a long duration, we

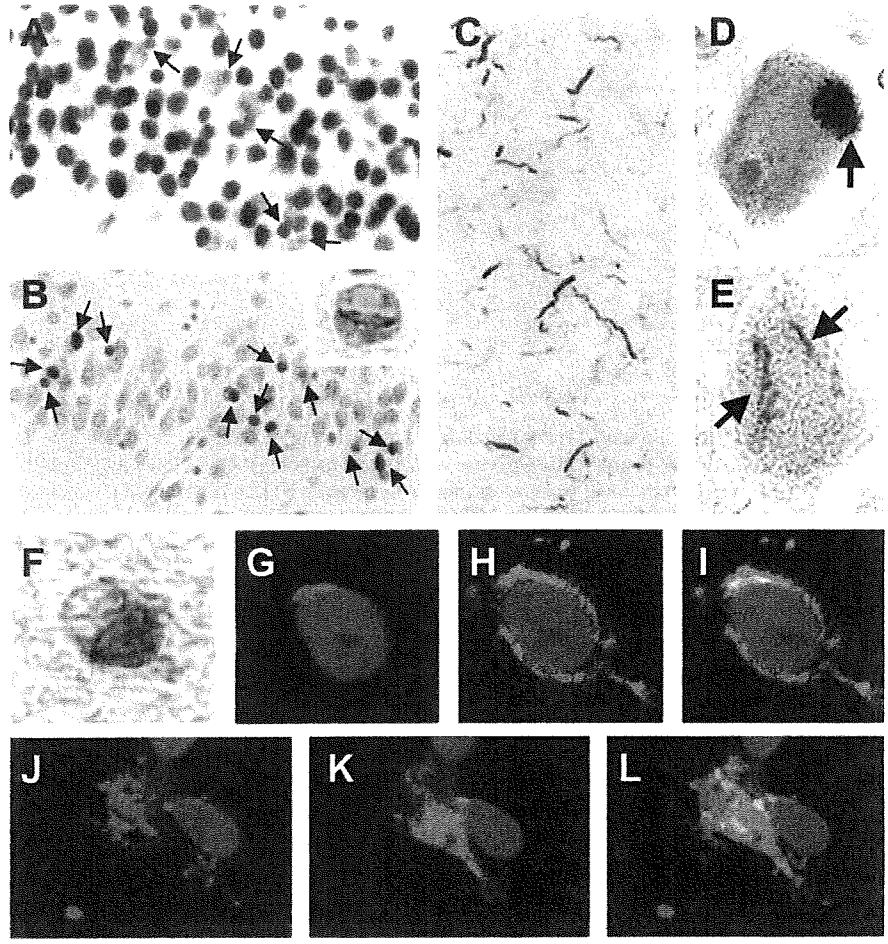


**Fig. 1** Neuronal and glial inclusions immunopositive for phosphorylated transactivation response (TAR) DNA-binding protein of Mr 43 kDa (TDP-43) in frontotemporal lobar degeneration (FTLD)-TDP and ALS. A. Dentate gyrus (DG) of the hippocampus of the FTLD-TDP case stained with the commercially available phosphorylation-independent anti-TDP-43 antibody. Both neuronal cytoplasmic inclusions (NCIs) (arrows) and normal neuronal nuclei are immunopositive. B. Dentate gyrus of the FTLD-TDP case stained with the pTDP-43-specific antibody (pS409/410). NCIs are clearly stained with no nuclear staining. Inset represents neuronal intranuclear inclusions with a cat-eye shape. C. Dystrophic neurites in the temporal cortex of the FTLD-TDP positive for pS409/410. Motoneuronal round inclusion (D) and skein-like inclusion (E) of the ALS case are stained with pS409/410. F. Glial cytoplasmic inclusions in the motor system of the ALS case stained with pS409/410. In double-label immunofluorescence histochemistry using pS409/410 (red in G, I) and anti-C4d (green in H, I), the pS409/410-positive inclusion (red) is present around the nucleus of the C4d-positive oligodendrocyte (green) (I). In the frontal cortex of the ALS case with long duration, double-label immunofluorescence using pS409/410 (red in J, L) and anti-GFAP (green in K, L) shows a partial colocalization of the both proteins in the cytoplasm of the astrocyte.

found a partial colocalization of pTDP-43 and GFAP in the cytoplasm of astrocytes (Fig. 1J–L). These results suggest that all of the inclusion types previously described in FTLD-TDP and ALS contain pTDP-43.

Immunoblot analyses of sarkosyl-insoluble fractions with pTDP-43-specific antibodies revealed a single band at 45 kDa, several smaller fragments at ~25 kDa and indistinct smears in FTLD-TDP and ALS cases but not in controls (Fig. 2A). The intensity of the ~25 kDa fragments tended to be greater than that of the 45 kDa band in FTLD-TDP and in ALS. All of the immunoreactive bands were completely abolished by lambda protein phosphatase treatment, proving the specificity of the antibodies to the phosphoepitopes.

To investigate the biochemical basis of the different TDP-43 pathological subtypes (Types 1–3), we carefully compared the results of immunoblots of the sarkosyl-insoluble fractions from the cerebral cortex of cases with sporadic FTLD-TDP (Type 1), FTLD-MND (Type 2), ALS (Type 2) and familial FTLD with *PGRN* mutations (m*PGRN*) (Type 3), using pTDP-43 specific antibodies. The results showed that there is a close relationship between the pathological subtypes and the immunoblot pattern of the 18–26 kDa C-terminal fragments of pTDP-43 (Fig. 2B,C). These findings confirm and extend the previous reports[1,31] that showed C-terminal fragment composition varied between cases with Type 1 and Type 2 pathology. Furthermore, these results parallel our earlier findings of differing C-terminal tau fragments in progressive supranuclear palsy and corticobasal degeneration, despite identical composition of tau isoforms.[39] Taken together, these results suggest that elucidating the mechanism of C-terminal fragment origination may shed light on the pathogenesis of several neurodegenerative disorders involving TDP-43 proteinopathy and tauopathy.

## TDP-43-POSITIVE STRUCTURES IN A VARIETY OF NEURODEGENERATIVE DISORDERS AND THE SUBCLASSIFICATION OF TDP-43 PROTEINOPATHY

Immunohistochemical examination, using commercially available phosphorylation-independent anti-TDP-43 antibodies, had demonstrated abnormal intracellular accumulation of TDP-43 in neurodegenerative disorders other

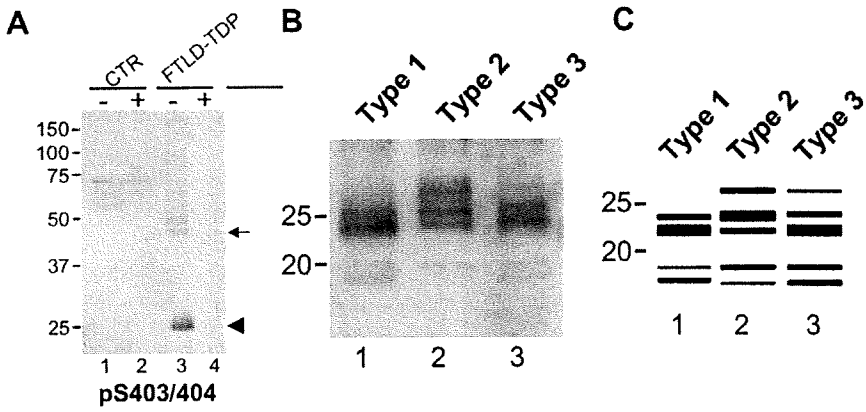


**Fig. 2** Biochemical analyses using antibodies specific for phosphorylated transactivation response (TAR) DNA-binding protein of Mr 43 kDa (pTDP-43). A. Immunoblot analyses of sarkosyl-insoluble fractions from control (lanes 1, 2) and frontotemporal lobar degeneration (FTLD)-TDP (lanes 3, 4), using pS403/404, before (−) and after (+) the treatment with lambda protein phosphatase. pS403/404 specifically label the ~45 kDa band (arrow) and the ~25 kDa fragments (arrowhead) as well as a smear, only in FTLD-TDP (lane 3). These immunoreactivities are abolished after dephosphorylation. B. Representative immunoblots with the pTDP-43 specific antibody, pS409/410. The sporadic FTLD-TDP case with Type 1 pathology shows two major bands at 23 and 24 kDa and two minor bands at 18 and 19 kDa (lane 1), while the FTLD-MND (motor neurone disease) case with Type 2 pathology shows three major bands at 23, 24 and 26 kDa and two minor bands at 18 and 19 kDa (lane 2). A 23 kDa band is the most intense in sporadic FTLD-TDP (lane 1), while a 24 kDa band is the most intense in FTLD-MND (lane 2). The band pattern of the case of familial FTLD with progranulin gene mutations with Type 3 pathology is not distinctive but intermediate between FTLD-TDP and FTLD-MND (lane 3). C. Schematic diagram showing the band pattern of the C-terminal fragments of pTDP-43.

than FTLD-TDP and ALS, including ALS/parkinsonism-dementia complex of Guam,[40–42] Alzheimer's disease (AD),[43–47] dementia with Lewy bodies (DLB),[44,48] Pick's disease,[2,49,50] hippocampal sclerosis,[43] and corticobasal degeneration (CBD).[47] However, the biochemical features of accumulated TDP-43, especially its phosphorylation sites and fragmentation, had been unclear in these disorders. To address these issues, we performed immunohistochemical and biochemical analyses of TDP-43 in cases of neurodegenerative disorders, using our pTDP-43-specific antibodies. As a result, we found a high frequency of pTDP-43 pathology in cases of AD (36–56%) (Fig. 3A,C), DLB (53–60%) (Fig. 3B,D), argyrophilic grain disease (AGD) (60%) (Fig. 3E), Huntington's disease (100%), and a case of familial British dementia.[51–54]

The pathological significance and mechanism of such a frequent co-occurrence of diverse protein aggregates are still unclear. A higher Braak NFT stage in the TDP-43-positive patients than in the TDP-43-negative ones was found in DLB+AD cases by Nakashima-Yasuda *et al.*[48] and in our study of AD cases.[51] We also reported parallel distribution of TDP-43-positive structures and tau-positive grains and higher AGD stages in cases with TDP-43 immunoreactivity than in those without TDP-43 immunoreactivity in AGD.[53] Double-label immunofluorescence microscopy reveals partial colocalization of tau and TDP-43 in AD, DLB, AGD, Guamanian PDC and CBD[40,41,43,44,47,48,53] or of α-synuclein and TDP-43 in DLB.[44,48,51] These findings suggest that there may be common factors or mechanisms that affect the conformation or modification of both proteins, leading to their intracellular accumulation. Nakashima-Yasuda *et al.* indicated two possibilities of the basis for those.[48] One is the direct interaction between the protein as tau and α-synuclein promote the fibrillization of each other *in vitro*.[55] The other is that the misfolding and aggregation of a disease protein disrupt normal cellular functions, leading to predisposing other proteins to aggregate.

**Table 1** Subclassification of TDP-43 proteinopathy

| | |
|---|---|
| 1. pure TDP-43 proteinopathy | |
| Disease | Gene (locus) |
| A. Familial | |
| FTDU-17 (FTLD-TDP, Type 3) | PGRN |
| IBMPFD (FTLD-TDP, Type 4) | VCP |
| Perry syndrome | DCTN1 |
| ALS | TARDBP (TDP-43) |
| FTLD-MND (FTLD-TDP, Type 2) | Chromosome 9 |
| B. Sporadic | |
| FTLD-TDP (Types 1-3) | |
| ALS | |
| 2. Combined TDP-43 proteinopathy | |
| Disease | Aggregated proteins |
| A. Familial | |
| FBD | ABri, Tau, TDP-43 |
| HD | Huntingtin, TDP-43 |
| MJD (SCA3) | Ataxin-3, TDP-43 |
| B. Sporadic | |
| AD | Tau, TDP-43 |
| DLB | Tau, Alpha-syn, TDP-43 |
| CBD | Tau, TDP-43 |
| AGD | Tau, TDP-43 |
| C. Endemic | |
| Guam ALS/PDC | Tau, Alpha-syn, TDP-43 |
| Kii ALS/PDC | Tau, Alpha-syn, TDP-43 |

FTDU-17, frontotemporal dementia with ubiquitinated inclusions linked to chromosome 17; PGRN, progranulin; IMBPFD, inclusion body myopathy associated with Paget disease of bone and frontotemporal dementia; DCTN1, dynactin 1; ALS, amyotrophic lateral sclerosis; TARDBP (TDP-43), TAR DNA-binding protein of 43 kDa.

AD, Alzheimer's disease; AGD, argyrophilic grain disease; Alpha-syn, α-synuclein; CBD, corticobasal degeneration; DLB, dementia with Lewy bodies; FBD, familial British dementia; FTLD-MND, frontotemporal lobar degeneration with motor neuron disease; HD, Huntington disease; MJD, Machado-Joseph disease; PDC, parkinsonism-dementia complex; SCA, Spinocerebellar ataxia.

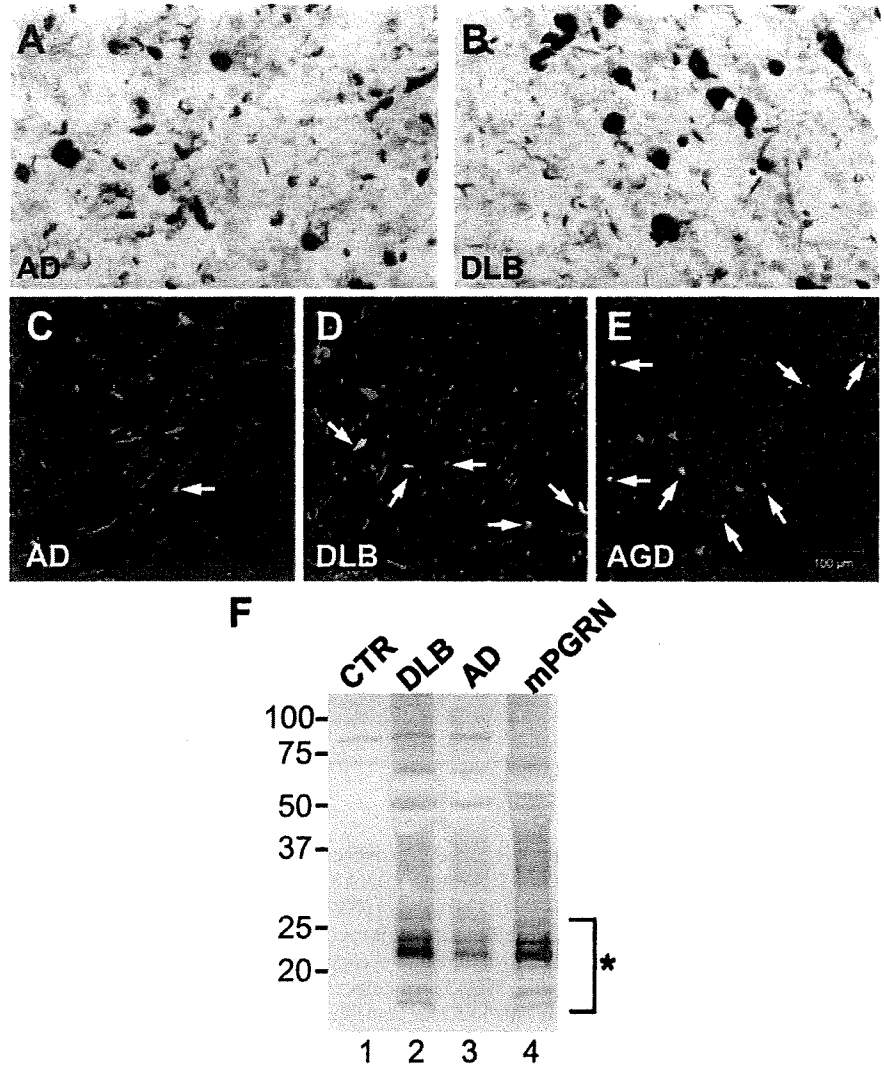


**Fig. 3** Phosphorylated transactivation response (TAR) DNA-binding protein of Mr 43 kDa (pTDP-43)-positive structures in other neurodegenerative disorders. A. Neuronal cytoplasmic inclusions (NCIs) and dystrophic neurites stained with the pTDP-43-specific antibody (pS403/404) in the temporal cortex of the Alzheimer's disease (AD) case (A) and the dementia with Lewy bodies (DLB) case (B) with diffuse TDP-43 pathology. (C–E) Double-label immunofluorescence histochemistry of the temporal cortex of AD (C) and DLB (D) and of the amygdala of argyrophilic grain disease (AGD) (E). The green fluorescence reveals the immunoreactivity for phosphorylated tau (AT8) in C and E, and that for phosphorylated α-synuclein in D, while the red fluorescence represents the immunopositivity for pS403/404 in C–E. Arrows indicate the colocalization of tau and pTDP-43 in C and E, and that of α-synuclein and pTDP-43 in D. F. The band pattern of the C-terminal fragments of pTDP-43 (asterisk) in DLB (lane 2) and AD (lane 3) is similar to that in familial FTLD with progranulin gene mutation (mPGRN).

Of the TDP-43-positive cases in AD and DLB, about 20–30% showed neocortical TDP-43 pathology resembling the FTLD-TDP, Type 3[51] (Fig. 3A,B). Immunoblot analyses of the sarkosyl-insoluble fraction from cases with neocortical TDP-43 pathology showed intense staining of several low-molecular-weight bands, corresponding to C-terminal fragments of TDP-43. Interestingly, the band pattern of these C-terminal fragments in AD and DLB also corresponds to that previously observed in the FTLD-TDP, Type 3[37] (Fig. 3F). These results suggest that the morphological and biochemical features of TDP-43 pathology are common between AD or DLB and a specific subtype of FTLD-TDP. Since all FTLD-TDP cases with PGRN mutations show Type 3 pathology,[56] there may be genetic factors, such as mutations or genetic variants of *PGRN* underlying the co-occurrence of abnormal deposition of TDP-43, tau and α-synuclein.

The clinical impact of the concurrent TDP-43 pathology in other neurodegenerative disorders than FTLD-TDP and ALS is also not fully understood. Uryu *et al.* reported a lack of association between TDP-43 pathology and clinical manifestation of AD.[47] Similarly, we did not find a significant difference of clinical features between AGD cases with and without TDP-43 pathology.[53] Joseph *et al.* on the other hand, reported that AD cases with TDP-43 pathology were older at onset and death, and performed worse on the Clinical Dementia Rating Scale, Mini-Mental State Examination, and Boston Naming Test than those without TDP-43 pathology.[46] The older age at death of the AD cases with TDP-43 pathology was also observed in our study.[51] Nakashima-Yasuda *et al.* found a higher average age at death in the TDP-43 positive cases in Lewy body-related diseases with dementia.[48] Further studies using larger cohorts with more detailed clinical, radiological and pathological data are needed to elucidate the clinical impact of TDP-43 pathology in a variety of neurodegenerative disorders.

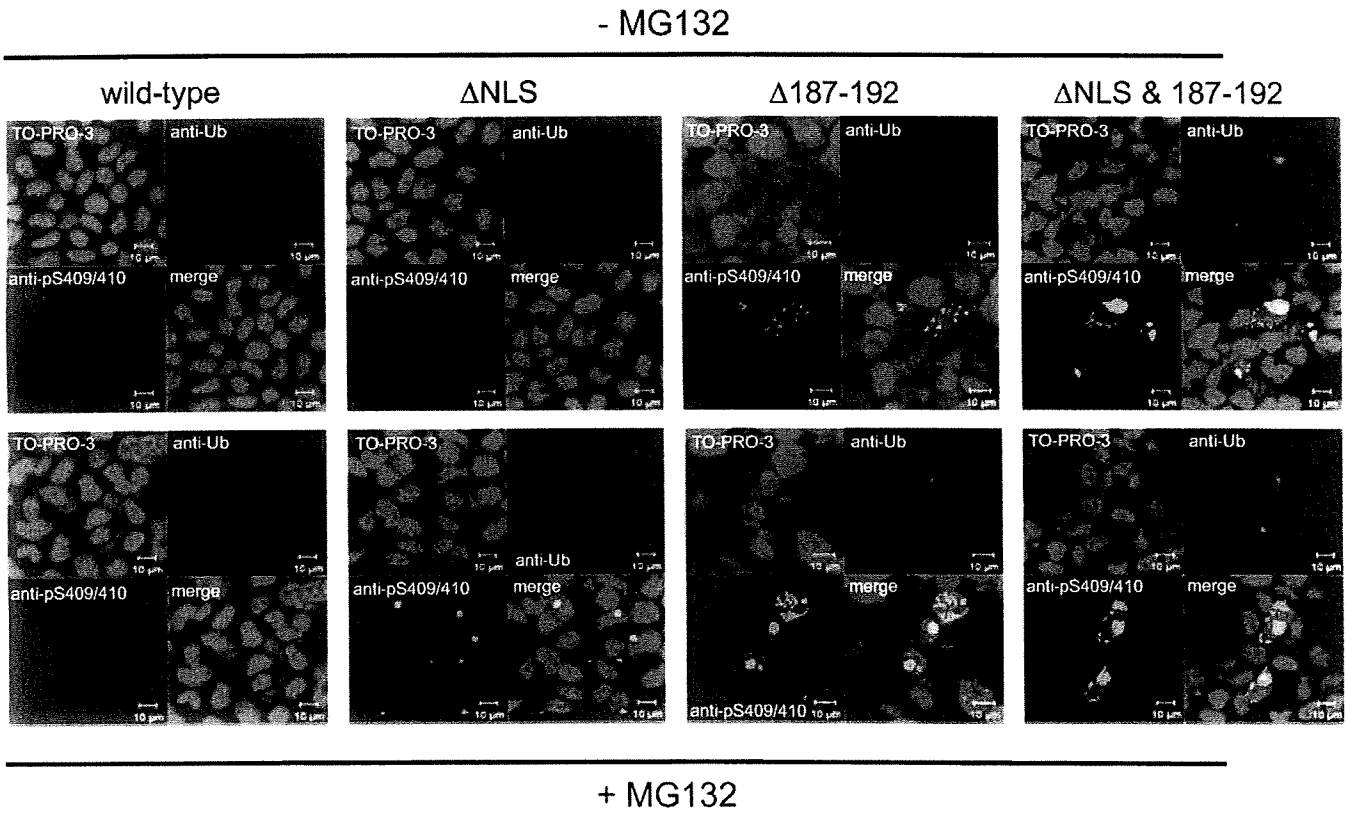


**Fig. 4** The formation of inclusion-like structures in cells transfected with deletion mutants of transactivation response (TAR) DNA-binding protein of Mr 43 kDa (TDP-43). When pcDNA3-TDP-43 wild-type was expressed in SH-SY5Y cells, no staining was observed by the phosphorylation-specific anti-TDP-43 antibody (pS409/410), indicating that transfected wild-type TDP-43 and endogenous TDP-43 are not phosphorylated at Ser409/410. The deletion mutant lacking nuclear localization signal (ΔNLS: 78–84 residues) was not recognized by pS409/410 without MG132 treatment, while round cytoplasmic inclusion-like structures were stained by both pS409/410 and anti-ubiquitin antibodies in those cells treated with MG132. In cells expressing another deletion mutant lacking 187–192 residues (Δ187–192), pS409/410-positive but ubiquitin-negative intranuclear dot-like structures were observed without treatment. With MG132, round intranuclear inclusions positive for pS409/410 and ubiquitin were formed. In cells expressing the double-deletion mutant (ΔNLS and 187–192), cytoplasmic inclusions positive for pS409/410 and ubiquitin were formed even in the absence of MG132.

Based on these findings so far, we would like to propose that TDP-43 proteinopathy can be divided into two groups (Table 1). One is "pure" TDP-43 proteinopathy, in which only TDP-43 accumulates in brains as a pathological protein. The other is "combined" TDP-43 proteinopathy, which shows multiple protein aggregates. TDP-43 pathology is always found in all cases of pure TDP-43 proteinopathy and familial and endemic cases of combined TDP-43 proteinopathy, while it is found in a subpopulation of cases with sporadic combined TDP-43 proteinopathy.

## ESTABLISHMENT AND ANALYSES OF CELLULAR MODELS OF TDP-43 PROTEINOPATHY

To establish the cellular models for intracellular aggregates of TDP-43, we first examined two candidate sequences for the nuclear localization signal (NLS) (Fig. 4).[57] Deletion of residues 78–84 resulted in cytoplasmic localization of TDP-43 in SH-SY5Y cells, proving that this sequence indeed functions as NLS. This result is largely consistent with the previous report by Winton *et al.* which showed that residues 82–98 were required for TDP-43 entry into the nucleus.[58] On the other hand, the mutant lacking residues 187–192 localized in nuclei, forming unique dot-like structures. Proteasome inhibition caused these to assemble into aggregates. Furthermore, double-deletion mutant of these sequences caused cytoplasmic inclusion formation without proteasomal inhibition. Immunohistochemical and immunoblot analyses showed that these inclusions consisted of phosphorylated and ubiquitinated TDP-43, suggesting that these cellular models recapitulate the phenotypes of TDP-43 proteinopathies both pathologically and biochemically.

Then, we tried to generate and analyze the cellular models by expressing C-terminal fragments of TDP-43 in

SH-SY5Y cells, since 18–26 kDa C-terminal fragments of TDP-43 are major constituents of inclusions in FTLD-TDP and ALS brains.[37] The results showed that expression of several TDP-43 C-terminal fragments as green fluorescent protein (GFP), including 162–414, 218–414, 219–414 and 247–414, led to the formation of cytoplasmic inclusions positive for pTDP-43 and ubiquitin (Fig. 5).[59] The N-termini of the latter two peptides, 219–414 and 247–414, correspond to the cleavage sites of TDP-43 C-terminal fragments accumulated in FTLD-TDP brains identified by our mass spectra analyses. Igaz *et al.* reported another cleavage site at Arg 208 in a pathological TDP-43 C-terminal fragment from FTLD-TDP brains and inclusion formation in cultured cells expressing resultant C-terminal fragment (residues 208–414).[60] Our immunoblot analysis showed that these aggregated pTDP-43 C-terminal fragments were recovered in sarkosyl-insoluble fraction as those in brains of FTLD-TDP and ALS.

Several groups have recently reported increased accumulation of TDP-43 fragments in the brain homogenates[13] and cultured cells[15,16] in some of the pathogenic mutations of TARDBP identified in ALS. However, in our cellular models, immunoblot analyses failed to show any significant differences in the generation of fragments of TDP-43 with or without various mutations. Alternatively, pathogenic mutations consistently enhanced aggregation of TDP-43 if they are present in the C-terminal fragment, GFP-TDP 162–414 (Fig. 6). These results suggest that pathogenic mutations and N-terminal truncation synergistically promote abnormal accumulation of TDP-43.

## METHYLENE BLUE AND DIMEBON INHIBIT AGGREGATION OF TDP-43 IN CELLULAR MODELS

Inhibition of the aggregation of TDP-43 and promotion of its clearance are considered to be major therapeutic avenues for ALS and FTLD-TDP. As for other neurodegenerative diseases, current tools include antibodies, synthetic peptides, molecular chaperones and chemical compounds. Of the latter, methylene blue (MB) and dimebon have recently been reported to have significant beneficial effects in phase II clinical trials of AD.[61,62] MB is a phenothiazine compound that has been used for treating methemoglobinemia,[63,64] inhibiting nitric oxide synthase,[65] reducing nGMP,[66] enhancing β-oxidation in mitochondria,[67] inhibiting of noradrenalin re-uptake[68] and enhancing brain mitochondrial cytochrome oxidase activity.[69,70] It has also been shown to inhibit AD-like Aβ and tau aggregation *in vitro*.[71,72] Dimebon is a non-selective antihistaminergic compound that was in clinical use for many years before more selective agents became available.[73] It has been reported to inhibit butyrylcholinesterase, acetylcholinesterase, NMDA receptors, voltage-gated calcium channels, adrenergic receptors, histamine H1 receptors, histamine H2 receptors and serotonin receptors, as well as to stabilize glutamate-induced Ca2+ signals.[74–76] The effects of dimebon on pathological protein aggregation have not been studied in detail.

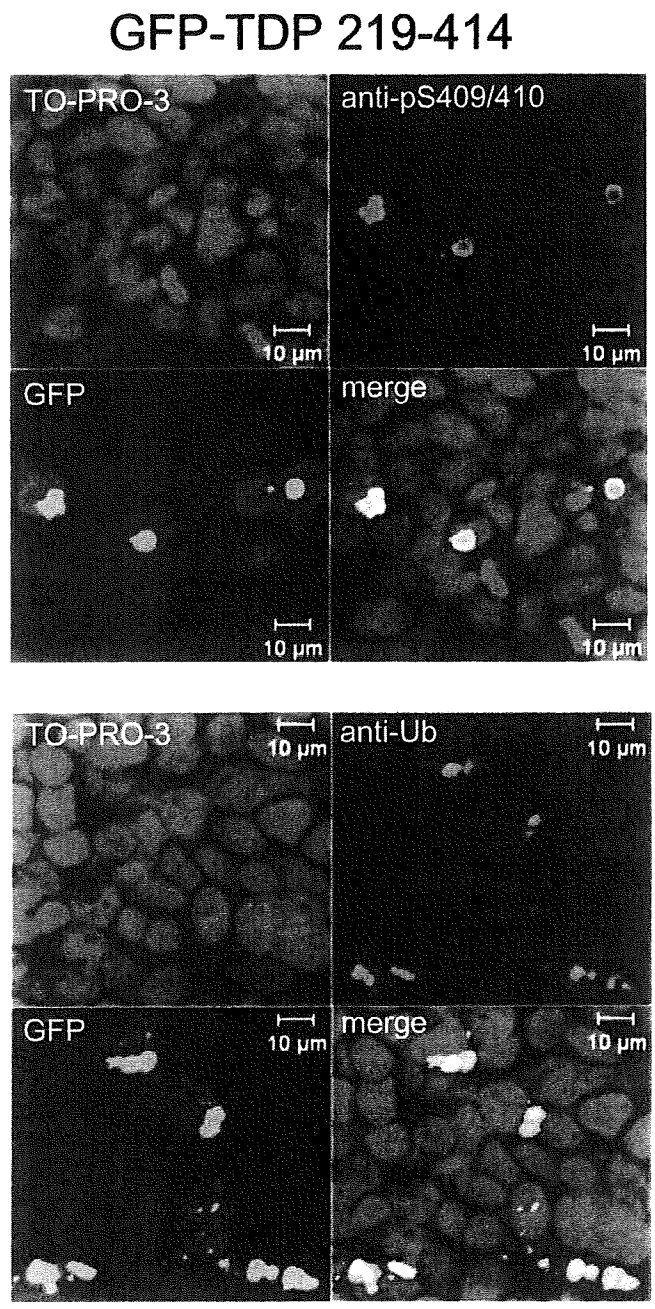


**Fig. 5** Transactivation response (TAR) DNA-binding protein of Mr 43 kDa (TDP-43) C-terminal fragments identified in diseased brains form cytoplasmic inclusions in cells. Round cytoplasmic inclusions with strong green fluorescent protein (GFP) intensities were observed in SH-SY5Y cells expressing GFP-TDP 219–414. These were positive for pS409/410 and ubiquitin Ub).

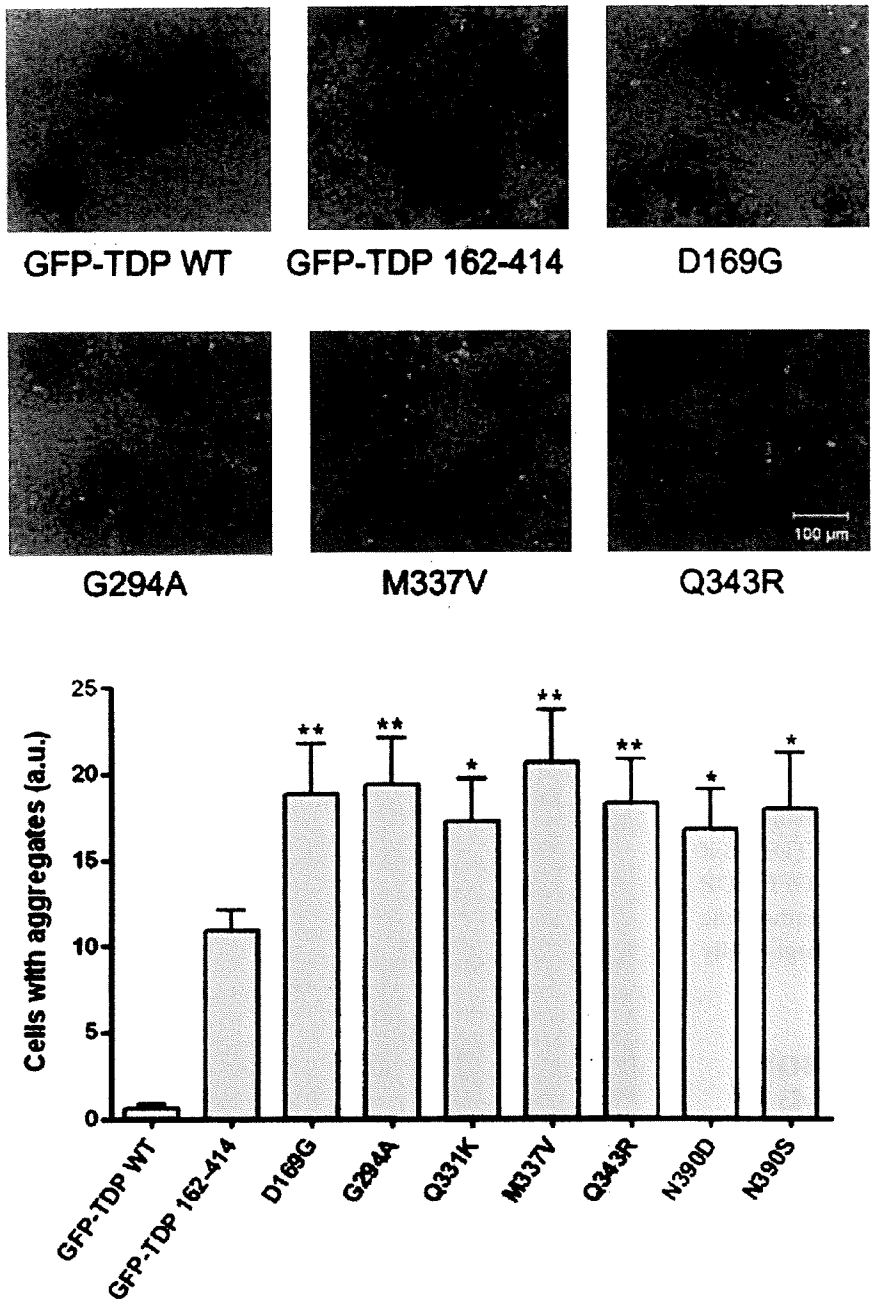


**Fig. 6** The effect of transactivation response (TAR) DNA-binding protein of Mr 43 kDa (TDP-43) mutations on aggregates formation of the C-terminal fragment of TDP-43. All seven mutations significantly facilitated the formation of intracellular aggregates of green fluorescent protein (GFP)-TDP 162–414, as compared with those of wild-type GFP-TDP 162–414.

Using our cellular models of TDP-43 proteinopathy described above, we investigated the effects of MB and dimebon on the formation of TDP-43 aggregates.[77] Following treatment with 0.05 μM MB or 5 μM dimebon, the number of TDP-43 aggregates was reduced by 50% and 45%, respectively (Fig. 7A–C,I). The combined use of MB and dimebon resulted in an 80% reduction in the number of aggregates (Fig. 7D,I), and in the significant reduction of phosphorylated TDP-43 in insoluble fraction of the cell lysate (Fig. 7E–H). These results suggest that MB and dimebon may be useful for the treatment of ALS, FTLD-TDP and other TDP-43 proteinopathies.

## CONCLUSION

Intracellular aggregation of TDP-43 takes place in brains of patients with ALS, FTLD and a variety of other neurodegenerative diseases, suggesting the possibility that TDP-43 has wide influence on neuronal dysfunction and neurodegeneration. Phosphorylated and truncated forms of TDP-43 are major species accumulated in diseased brains, and the proteolytic cleavage of TDP-43 may play an important role for the pathological process of TDP-43 proteinopathy. In cultured cells, expression of the TDP-43 C-terminal fragments results in accelerated aggregate formation and in

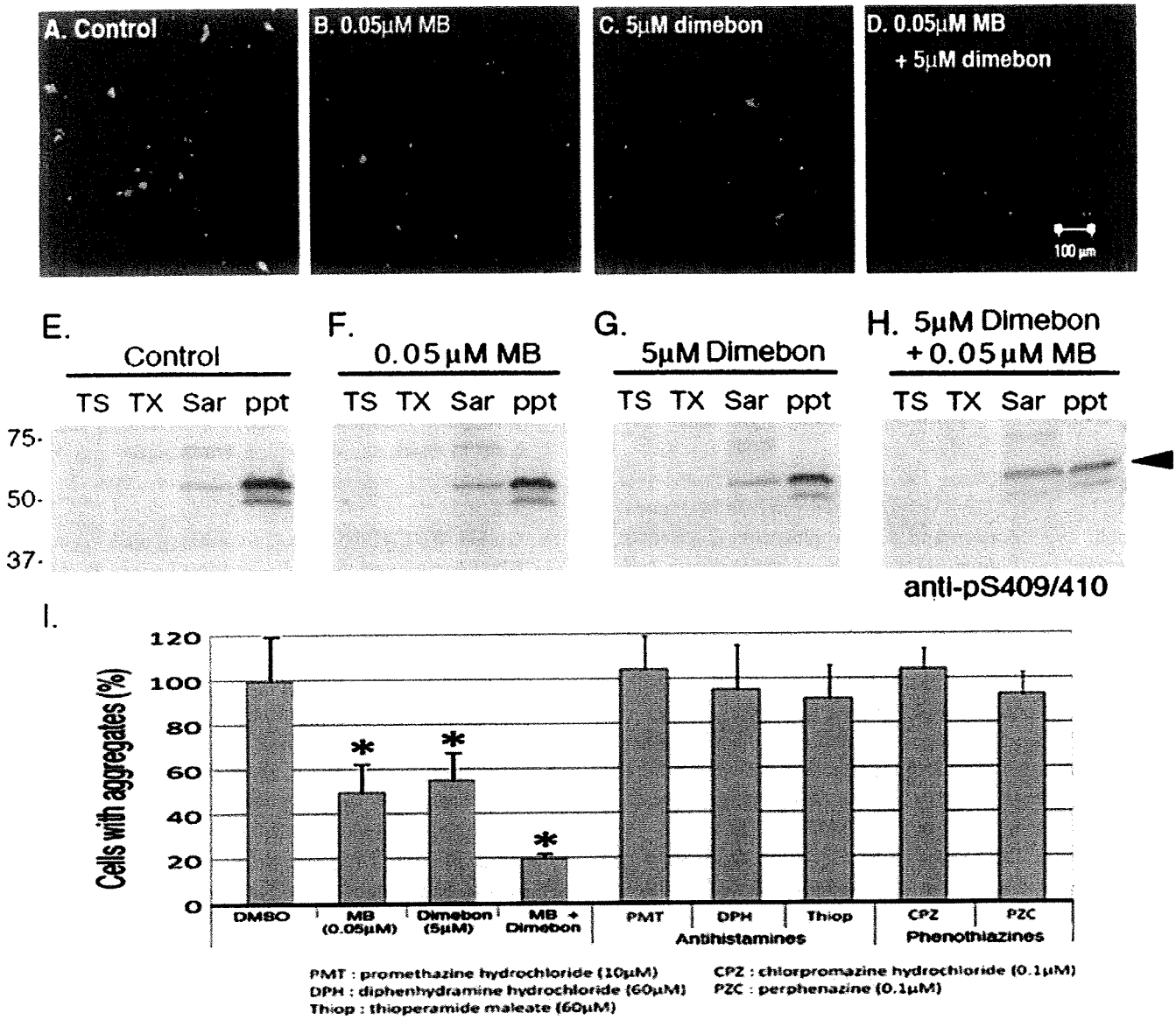


**Fig. 7** Inhibition of aggregates formation of transactivation response (TAR) DNA-binding protein of Mr 43 kDa (TDP-43) in cellular models by methylene blue (MB) and dimebon. (A–D) Immunohistochemical analysis of the effects of MB and dimebon on the aggregation of TDP-43 in SH-SY5Y cells expressing TDP-43 (ΔNLS and 187–192). TDP-43 inclusions were stained with anti-pS409/410 antibody and detected with Alexa Fluor 488-labeled secondary antibody. Representative confocal images from cells treated with control (dimethyl sulfoxide + distilled water) (A), 0.05 μM MB (B), 5 μM dimebon (C) and 0.05 μM MB + 5 μM dimebon (D) are shown. (E–H): Immunoblot analysis of the effects of MB and dimebon on the aggregation of TDP-43 in SH-SY5Y cells expressing green fluorescent protein (GFP)-tagged TDP-43 C-terminal fragment (162–414). Tris saline (TS)-soluble material, Triton X-100 (TX)-soluble material, Sarkosyl (Sar)-soluble material and the remaining pellet (ppt) were prepared from control cells (E) and from cells treated with 0.05 μM MB (F), 5 μM dimebon (G), and 0.05 μM MB + 5 μM dimebon (H), run on SDS-PAGE and immunoblotted with anti-pS409/410 antibody. (I) Quantitation of cells with TDP-43 aggregates. The number of cells with intracellular TDP-43 aggregates was counted and expressed as the percentage of cells with aggregates in the absence of compound (taken as 100%). Data are means ± SEM $*P < 0.01$ by Student's *t*-test.

failure of nuclear localization of endogenous TDP-43. At present, it is unknown whether loss of function, toxic gain of function, or a combination of both mechanisms contributes to neurodegeneration. Cultured cells or animal models expressing those abnormal TDP-43 species are expected to be useful tools to investigate the pathogenesis of TDP-43 proteinopathy and to develop effective diagnostics and therapeutics.

## REFERENCES


1. Neumann M, Sampathu DM, Kwong LK *et al.* Ubiquitinated TDP-43 in frontotemporal lobar degeneration and amyotrophic lateral sclerosis. *Science* 2006; **314**: 130–133.
2. Arai T, Hasegawa M, Akiyama H *et al.* TDP-43 is a component of ubiquitin-positive tau-negative inclusions in frontotemporal lobar degeneration and amyotrophic lateral sclerosis. *Biochem Biophys Res Commun* 2006; **351**: 602–611.
3. Davidson Y, Kelley T, Mackenzie IRA *et al.* Ubiquitinated pathological lesions in frontotemporal lobar degeneration contain the TAR DNA-binding protein, TDP-43. *Acta Neuropathol (Berl)* 2007; **113**: 521–533.
4. Neumann M, Kwong LK, Sampathu DM, Trojanowski JQ, Lee VM. TDP-43 proteinopathy in frontotemporal lobar degeneration and amyotrophic lateral sclerosis: protein misfolding diseases without amyloidosis. *Arch Neurol* 2007; **64**: 1388–1394.
5. Mackenzie IR, Bigio EH, Ince PG *et al.* Pathological TDP-43 distinguishes sporadic amyotrophic lateral sclerosis from amyotrophic lateral sclerosis with SOD1 mutations. *Ann Neurol* 2007; **61**: 427–434.
6. Tan CF, Eguchi H, Tagawa A *et al.* TDP-43 immunoreactivity in neuronal inclusions in familial amyotrophic lateral sclerosis with or without SOD1 gene mutation. *Acta Neuropathol (Berl)* 2007; **113**: 535–542.
7. Mackenzie IR, Neumann M, Bigio EH *et al.* Nomenclature for neuropathologic subtypes of frontotemporal lobar degeneration: consensus recommendations. *Acta Neuropathol* 2009; **117**: 15–18.
8. Baker M, Mackenzie IR, Pickering-Brown SM *et al.* Mutations in progranulin cause tau-negative frontotemporal dementia linked to chromosome 17. *Nature* 2006; **442**: 916–919.
9. Cruts M, Gijselinck I, van der Zee J *et al.* Null mutations in progranulin cause ubiquitin-positive frontotemporal dementia linked to chromosome 17q21. *Nature* 2006; **442**: 920–924.
10. Watts GDJ, Wymer J, Kovach MJ *et al.* Inclusion body myopathy associated with Paget disease of bone and frontotemporal dementia is caused by mutant valosin-containing protein. *Nat Genet* 2004; **36**: 377–381.
11. Morita M, Al-Chalabi A, Anderson PM *et al.* A locus on chromosome 9p confers susceptibility to ALS and frontotemporal dementia. *Neurology* 2006; **66**: 839–844.
12. Vance C, Al-Chalabi A, Ruddy D *et al.* Familial amyotrophic lateral sclerosis with frontotemporal dementia is linked to a locus on chromosome 9p13.2-21.3. *Brain* 2006; **129**: 868–875.
13. Yokoseki A, Shiga A, Tan CF *et al.* TDP-43 Mutation in Familial Amyotrophic Lateral Sclerosis. *Ann Neurol* 2008; **63**: 538–542.
14. Gitcho MA, Baloh RH, Chakraverty S *et al.* TDP-43 A315T mutation in familial motor neuron disease. *Ann Neurol* 2008; **63**: 535–538.
15. Sreedharan J, Blair IP, Tripathi VB *et al.* TDP-43 mutations in familial and sporadic amyotrophic lateral sclerosis. *Science* 2008; **319**: 1668–1672.
16. Kabashi E, Valdmanis PN, Dion P *et al.* TARDBP mutations in individuals with sporadic and familial amyotrophic lateral sclerosis. *Nat Genet* 2008; **40**: 572–574.
17. Van Deerlin VM, Leverenz JB, Bekris LM *et al.* TARDBP mutations in amyotrophic lateral sclerosis with TDP-43 neuropathology: a genetic and histopathological analysis. *Lancet Neurol* 2008; **7**: 409–416.
18. Ou SH, Wu F, Harrich D, Garcia-Martinez LF, Gaynor RB. Cloning and characterization of a novel cellular protein, TDP-43, that binds to human immunodeficiency virus type 1 TAR DNA sequence motifs. *J Virol* 1995; **69**: 3584–3596.
19. Wang H-Y, Wang I-F, Bose J, Shen C-KJ. Structural diversity and functional implications of the eukaryotic TDP gene family. *Genomics* 2004; **83**: 130–139.
20. Abhyankar MM, Urekar C, Reddi PP. A novel CpG-free vertebrate insulator silences the testis-specific SP-10 gene in somatic tissues: role for TDP-43 in insulator function. *J Biol Chem* 2007; **282**: 36143–36154.
21. Strong MJ, Volkening K, Hammond R *et al.* TDP43 is a human low molecular weight neurofilament (hNFL) mRNA-binding protein. *Mol Cell Neurosci* 2007; **35**: 320–327.
22. Ayala YM, Misteli T, Baralle FE. TDP-43 regulates retinoblastoma protein phosphorylation through the repression of cyclin-dependent kinase 6 expression. *Proc Natl Acad Sci USA* 2008; **105**: 3785–3789.
23. Buratti E, Baralle FE. Characterization and functional implications of the RNA binding properties of nuclear factor TDP-43, a novel splicing regulator of CFTR exon 9. *J Biol Chem* 2001; **276**: 36337–36343.
24. Buratti E, Dork T, Zuccato E, Pagani F, Romano M, Baralle FE. Nuclear factor TDP-43 and SR proteins promote in vitro and in vivo CFTR exon 9 skipping. *EMBO J* 2001; **20**: 1774–1784.
25. Mercado PA, Ayala YM, Romano M, Buratti E, Baralle FE. Depletion of TDP 43 overrides the need for exonic and intronic splicing enhancers in the human apoA-II gene. *Nucleic Acids Res* 2005; **33**: 6000–6010.
26. Bose JK, Wang IF, Hung L, Tarn WY, Shen CK. TDP-43 overexpression enhances exon 7 inclusion

during the survival of motor neuron pre-mRNA splicing. *J Biol Chem* 2008; **283**: 28852–28859.
27. Buratti E, Brindisi A, Giombi M, Tisminetzky S, Ayala YM, Baralle FE. TDP-43 binds heterogeneous nuclear ribonucleoprotein A/B through its C-terminal tail. *J Biol Chem* 2005; **280**: 37572–37584.
28. Buratti E, Baralle FE. Multiple roles of TDP-43 in gene expression, splicing regulation, and human disease. *Front Biosci* 2008; **13**: 867–878.
29. Mackenzie IRA, Baborie A, Pickering-Brown S *et al.* Heterogeneity of ubiquitin pathology in frontotemporal lobar degeneration: classification and relation to clinical phenotype. *Acta Neuropathol (Berl)* 2006; **112**: 539–549.
30. Mackenzie IRA, Baker M, Pickering-Brown S *et al.* The neuropathology of frontotemporal lobar degeneration caused by mutations in the progranulin gene. *Brain* 2006; **129**: 3081–3090.
31. Sampathu DM, Neumann M, Kwong LK *et al.* Pathological heterogeneity of frontotemporal lobar degeneration with ubiquitin-positive inclusions delineated by ubiquitin immunohistochemistry and novel monoclonal antibodies. *Am J Pathol* 2006; **169**: 1343–1352.
32. Cairns NJ, Bigio EH, Mackenzie IR *et al.* Neuropathologic diagnostic and nosologic criteria for frontotemporal lobar degeneration: consensus of the Consortium for Frontotemporal Lobar Degeneration. *Acta Neuropathol (Berl)* 2007; **114**: 5–22.
33. Snowden J, Neary D, Mann D. Frontotemporal lobar degeneration: clinical and pathological relationships. *Acta Neuropathol (Berl)* 2007; **114**: 31–38.
34. Kwong LK, Uryu K, Trojanowski JQ, Lee VM. TDP-43 proteinopathies: neurodegenerative protein misfolding diseases without amyloidosis. *Neurosignals* 2008; **16**: 41–51.
35. Geser F, Brandmeir NJ, Kwong LK *et al.* Evidence of multisystem disorder in whole-brain map of pathological TDP-43 in amyotrophic lateral sclerosis. *Arch Neurol* 2008; **65**: 636–641.
36. Nishihira Y, Tan CF, Hoshi Y *et al.* Sporadic amyotrophic lateral sclerosis of long duration is associated with relatively mild TDP-43 pathology. *Acta Neuropathol* 2009; **117**: 45–53.
37. Hasegawa M, Arai T, Nonaka T *et al.* Phosphorylated TDP-43 in frontotemporal lobar degeneration and amyotrophic lateral sclerosis. *Ann Neurol* 2008; **64**: 60–70.
38. Inukai Y, Nonaka T, Arai T *et al.* Abnormal phosphorylation of Ser409/410 of TDP-43 in FTLD-U and ALS. *FEBS Lett* 2008; **582**: 2899–2904.
39. Arai T, Ikeda K, Akiyama H *et al.* Identification of amino-terminally cleaved tau fragments that distinguish progressive supranuclear palsy from corticobasal degeneration. *Ann Neurol* 2004; **55**: 72–79.
40. Hasegawa M, Arai T, Akiyama H *et al.* TDP-43 is deposited in the Guam parkinsonism-dementia complex brains. *Brain* 2007; **130**: 1386–1394.
41. Geser F, Winton MJ, Kwong LK *et al.* Pathological TDP-43 in parkinsonism-dementia complex and amyotrophic lateral sclerosis of Guam. *Acta Neuropathol (Berl)* 2007; **115**: 133–145.
42. Miklossy J, Steele JC, Yu S *et al.* Enduring involvement of tau, beta-amyloid, alpha-synuclein, ubiquitin and TDP-43 pathology in the amyotrophic lateral sclerosis/parkinsonism-dementia complex of Guam (ALS/PDC). *Acta Neuropathol* 2008; **116**: 625–637.
43. Amador-Ortiz C, Lin WL, Ahmed Z *et al.* TDP-43 immunoreactivity in hippocampal sclerosis and Alzheimer's disease. *Ann Neurol* 2007; **61**: 435–445.
44. Higashi S, Iseki E, Yamamoto R *et al.* Concurrence of TDP-43, tau and alpha-synuclein pathology in brains of Alzheimer's disease and dementia with Lewy bodies. *Brain Res* 2007; **1184**: 284–294.
45. Hu WT, Josephs KA, Knopman DS *et al.* Temporal lobar predominance of TDP-43 neuronal cytoplasmic inclusions in Alzheimer disease. *Acta Neuropathol* 2008; **116**: 215–220.
46. Josephs KA, Whitwell JL, Knopman DS *et al.* Abnormal TDP-43 immunoreactivity in AD modifies clinicopathologic and radiologic phenotype. *Neurology* 2008; **70**: 1850–1857.
47. Uryu K, Nakashima-Yasuda H, Forman MS *et al.* Concomitant TAR-DNA-binding protein 43 pathology is present in Alzheimer disease and corticobasal degeneration but not in other tauopathies. *J Neuropathol Exp Neurol* 2008; **67**: 555–564.
48. Nakashima-Yasuda H, Uryu K, Robinson J *et al.* Co-morbidity of TDP-43 proteinopathy in Lewy body related diseases. *Acta Neuropathol (Berl)* 2007; **114**: 221–229.
49. Freeman SH, Spires-Jones T, Hyman BT, Growdon JH, Frosch MP. TAR-DNA binding protein 43 in Pick disease. *J Neuropathol Exp Neurol* 2008; **67**: 62–67.
50. Lin WL, Dickson DW. Ultrastructural localization of TDP-43 in filamentous neuronal inclusions in various neurodegenerative diseases. *Acta Neuropathol* 2008; **116**: 205–213.
51. Arai T, Mackenzie IR, Hasegawa M *et al.* Phosphorylated TDP-43 in Alzheimer's disease and dementia with Lewy bodies. *Acta Neuropathol* 2009; **117**: 125–136.
52. Schwab C, Arai T, Hasegawa M, Akiyama H, Yu S, McGeer PL. TDP-43 pathology in familial British dementia. *Acta Neuropathol* 2009; **118**:303–311.
53. Fujishiro H, Uchikado H, Arai T *et al.* Accumulation of phosphorylated TDP-43 in brains of patients with

argyrophilic grain disease. *Acta Neuropathol* 2009; **117**: 151–158.
54. Schwab C, Arai T, Hasegawa M, Yu S, McGeer PL. Colocalization of transactivation-responsive DNA-binding protein 43 and huntingtin in inclusions of Huntington disease. *J Neuropathol Exp Neurol* 2008; **67**: 1159–1165.
55. Giasson BI, Forman MS, Higuchi M *et al.* Initiation and synergistic fibrillization of tau and alpha-synuclein. *Science* 2003; **300**: 636–640.
56. Cairns NJ, Neumann M, Bigio EH *et al.* TDP-43 in familial and sporadic frontotemporal lobar degeneration with ubiquitin inclusions. *Am J Pathol* 2007; **171**: 227–240.
57. Nonaka T, Arai T, Buratti E, Baralle FE, Akiyama H, Hasegawa M. Phosphorylated and ubiquitinated TDP-43 pathological inclusions in ALS and FTLD-U are recapitulated in SH-SY5Y cells. *FEBS Lett* 2009; **583**: 394–400.
58. Winton MJ, Igaz LM, Wong MM, Kwong LK, Trojanowski JQ, Lee VM. Disturbance of nuclear and cytoplasmic TAR DNA-binding protein (TDP-43) induces disease-like redistribution, sequestration, and aggregate formation. *J Biol Chem* 2008; **283**: 13302–13309.
59. Nonaka T, Kametani F, Arai T, Akiyama H, Hasegawa M. Truncation and pathogenic mutations facilitate the formation of intracellular aggregates of TDP-43. *Hum Mol Genet* 2009; **18**: 3353–3364.
60. Igaz LM, Kwong LK, Chen-Plotkin A *et al.* Expression of TDP-43 C-terminal Fragments in Vitro Recapitulates Pathological Features of TDP-43 Proteinopathies. *J Biol Chem* 2009; **284**: 8516–8524.
61. Gura T. Hope in Alzheimer's fight emerges from unexpected places. *Nat Med* 2008; **14**: 894.
62. Doody RS, Gavrilova SI, Sano M *et al.* Effect of dimebon on cognition, activities of daily living, behaviour, and global function in patients with mild-to-moderate Alzheimer's disease: a randomized, double-blind, placebo-controlled study. *Lancet* 2008; **372**: 207–215.
63. Kristiansen JE. Dyes, antipsychotic drugs, and antimicrobial activity. Fragments of a development, with special reference to the influence of Paul Ehrlich. *Dan Med Bull* 1989; **36**: 178–185.
64. Mansouri A, Lurie AA. Concise review: methemoglobinemia. *Am J Hematol* 1993; **42**: 7–12.
65. Faber P, Ronald A, Millar BW. Methylthioninium chloride: pharmacology and clinical applications with special emphasis on nitric oxide mediated vasodilatory shock during cardiopulmonary bypass. *Anaesthesia* 2005; **60**: 575–587.
66. Heiberg IL, Wegener G, Rosenberg R. Reduction of cGMP and nitric oxide has antidepressant-like effects in the forced swimming test in rats. *Behav Brain Res* 2002; **134**: 479–484.
67. Visarius TM, Stucki JW, Lauterburg BH. Stimulation of respiration by methylene blue in rat liver mitochondria. *FEBS Lett* 1997; **412**: 157–160.
68. Chies AB, Custodio RC, de Souza GL, Correa FM, Pereira OC. Pharmacological evidence that methylene blue inhibits noradrenaline neuronal uptake in the rat vas deferens. *Pol J Pharmacol* 2003; **55**: 573–579.
69. Wrubel KM, Riha PD, Maldonado MA, McCollum D, Gonzalez-Lima F. The brain metabolic enhancer methylene blue improves discrimination learning in rats. *Pharmacol Biochem Behav* 2007; **86**: 712–717.
70. Atamna H, Nguyen A, Schultz C *et al.* Methylene blue delays cellular senescence and enhances key mitochondrial biochemical pathways. *Faseb J* 2008; **22**: 703–712.
71. Wischik CM, Edwards PC, Lai RY, Roth M, Harrington CR. Selective inhibition of Alzheimer disease-like tau aggregation by phenothiazines. *Proc Natl Acad Sci USA* 1996; **93**: 11213–11218.
72. Taniguchi S, Suzuki N, Masuda M *et al.* Inhibition of heparin-induced tau filament formation by phenothiazines, polyphenols, and porphyrins. *J Biol Chem* 2005; **280**: 7614–7623.
73. Burns A, Jacoby R. Dimebon in Alzheimer's disease: old drug for new indication. *Lancet* 2008; **372**: 179–180.
74. Bachurin S, Bukatina E, Lermontova N *et al.* Antihistamine agent Dimebon as a novel neuroprotector and a cognition enhancer. *Ann N Y Acad Sci* 2001; **939**: 425–435.
75. Wu J, Li Q, Bezprozvanny I. Evaluation of Dimebon in cellular model of Huntington's disease. *Mol Neurodegener* 2008; **3**: 15.
76. Lermontova NN, Redkozubov AE, Shevtsova EF, Serkova TP, Kireeva EG, Bachurin SO. Dimebon and tacrine inhibit neurotoxic action of beta-amyloid in culture and block L-type Ca(2+) channels. *Bull Exp Biol Med* 2001; **132**: 1079–1083.
77. Yamashita M, Nonaka T, Arai T *et al.* Methylene blue and dimebon inhibit aggregation of TDP-43 in cellular models. *FEBS Lett* 2009; **583**: 2419–2424.

# Myeloperoxidase antineutrophil cytoplasmic antibody–associated vasculitis with diffuse tubulointerstitial nephritis

**Daisuke Son[1], Hiroko Kanda[2], Akihiro Yamaguchi[2], Kimito Kawabata[2], Takahisa Kawakami[1], Kanae Kubo[2], Mana Higashihara[3], Jun Shimizu[3], Hiroshi Uozaki[4], Shigeru Kuramochi[5], Yoshikata Misaki[2], Fujio Takeuchi[2], Kazuhiko Yamamoto[2]**

[1]Department of Nephrology and Endocrinology, University of Tokyo, Tokyo - Japan
[2]Department of Allergy and Rheumatology, University of Tokyo, Tokyo - Japan
[3]Department of Neurology, University of Tokyo, Tokyo - Japan
[4]Department of Pathology, University of Tokyo, Tokyo - Japan
[5]Department of Pathology, National Tokyo Medical Center, Tokyo - Japan

## ABSTRACT

**Renal involvement in antineutrophil cytoplasmic antibody (ANCA)–associated vasculitis is characterized by focal segmental crescentic and/or necrotizing glomerulonephritis. Here, we report the case of a 66-year-old woman showing myeloperoxidase (MPO)–ANCA positivity and mononeuritis multiplex whose kidney biopsy revealed severe and diffuse tubulointerstitial nephritis despite the fact that crescentic necrotizing glomerulonephritis was focal. The mechanism of tubulointerstitial injury in ANCA-associated vasculitis remains unclear. Further studies are necessary to confirm the relationship between diffuse tubulointerstitial nephritis and ANCA-associated vasculitis.**

**Key words:** *ANCA, Interstitial nephritis, Mononeuritis multiplex, Vasculitis*

## INTRODUCTION

Antineutrophil cytoplasmic antibody (ANCA)–associated vasculitis includes many disease entities such as microscopic polyangiitis, Churg-Strauss syndrome and Wegener's granulomatosis, and its renal involvement often shows crescentic necrotizing glomerulonephritis. However, diffuse tubulointerstitial nephritis associated with ANCA-associated vasculitis has seldom been reported, except for some cases such as those of granulomatous tubulointerstitial nephritis in Wegener's granulomatosis (1). Recently, we have encountered a patient with myeloperoxidase (MPO) ANCA–associated vasculitis whose kidney biopsy revealed diffuse tubulointerstitial nephritis despite the fact that crescentic necrotizing glomerulonephritis was focal, which suggests the importance of evaluating tubulointerstitial changes in systemic vasculitis.

## CASE REPORT

A 66-year-old woman was referred to a local hospital by her primary physician for the evaluation of low-grade fever and lower left leg pain with exercise. She had had these symptoms for 1 month, and had general fatigue and loss of appetite. A peripheral blood test showed an elevated C-reactive protein (CRP) level (6.3 mg/dL), and she was treated with intravenous antibiotics (ampicillin and sulbactam, and ceftazidime) for 2 weeks and prescribed nonsteroidal anti-inflammatory drugs (NSAIDs); however, her symptoms did not improve. Because data such as elevated antinuclear antibody (ANA) (1:160) and rheumatoid factor (RF: 98.9 IU/L) levels suggested the presence of autoimmune disease, she was prescribed oral prednisone (30 mg/day). Her condition rapidly improved to show a normal temperature and a normal CRP level, and oral prednisone was tapered and discontinued within 1 month.

Several weeks after the discontinuation of oral prednisone, low-grade fever and general fatigue relapsed and resulted in a loss of 5 kg body weight. Therefore, she was referred

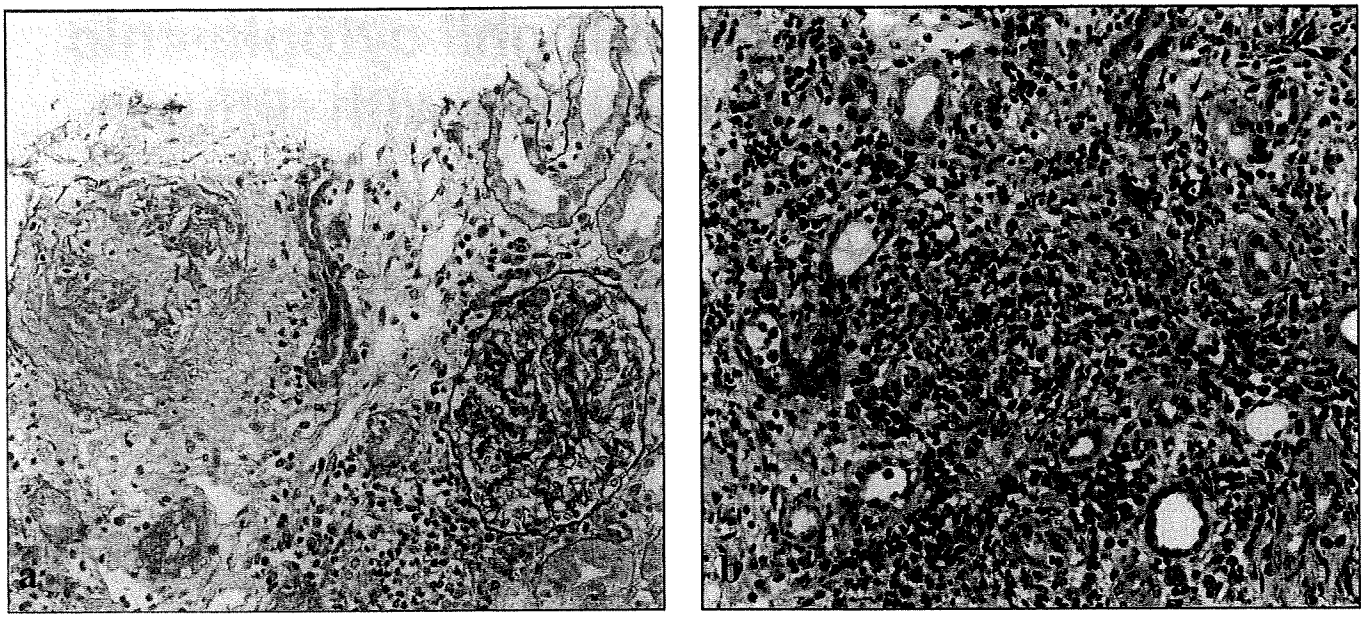

**Fig. 1 - Renal pathology. a) The left glomerulus in which fibrocellular crescent and mostly normal glomeruli are shown (periodic acid-Schiff staining, magnification ×200). b) A severe infiltration of inflammatory cells including neutrophils, lymphocytes, plasmacytes and occasional eosinophils is shown in the vast area of the interstitium (periodic acid-Schiff staining, magnification ×200).**

to our hospital. Physical examination revealed scattered small purpura (3 mm in diameter) associated with motor and sensory disturbance in the area of the left deep peroneal nerve. Her past history included allergic rhinitis and hypertension for which she had been prescribed an antihypertensive drug for 2 years. Hematological examination revealed leukocytosis of 9,800 cells/μL with 7% eosinophils (686/μL) and anemia with a hemoglobin level of 7.9 g/dL. Her serum CRP level was 4 mg/dL, and her erythrocyte sedimentation rate was 99 mm/hour. The MPO-ANCA titer was elevated up to 182 EU, whereas proteinase 3–ANCA, anti-dsDNA and anti-glomerular basement membrane antibodies were all negative. The RF level was as high as 479 IU/L, ANA was negative and serum complement levels were within the normal limits. Blood urea nitrogen level was 25 mg/dL, and creatinine level was 1.5 mg/dL. Creatinine clearance was 40.5 ml/min. A urinalysis revealed mild proteinuria (480 mg/day) and microhematuria (6-10 red blood cells per high-power field) with white blood cell and granular cast formation. Urinary $\alpha_1$-microglobulin and *N*-acetyl-β-d-glucosaminide levels were elevated to 69 mg/g creatinine and 16 IU/day, respectively. A skin biopsy from the lower left leg purpura showed a marked infiltration of inflammatory cells around medium-sized arteries (about 250 μm in diameter). Electromyography revealed a neurogenic pattern in the left peroneal nerve. A biopsy from the left peroneus brevis muscle and left sural nerve showed necrotizing vasculitis of medium-sized arteries (about 150 μm in diameter) with fibrinoid necrosis and acute axonal degeneration of most myelinated fibers, which is compatible with the diagnosis of mononeuritis multiplex.

On the eighth day of hospitalization, a needle biopsy of the kidney was performed. One of the 15 glomeruli obtained showed global sclerosis. Fibrocellular crescent formation and segmental necrotizing lesion were observed in 5 glomeruli; the other glomeruli were intact (Fig. 1a). The interstitium was severely and diffusely infiltrated by various inflammatory cells including neutrophils, lymphocytes, plasmacytes and a few eosinophils (Fig. 1b). In addition, typical findings of tubulitis were diffusely detected. No signs of necrotizing arteritis were noted. Immunofluorescence staining for immunoglobulins or complements was negative.

The diagnosis of ANCA-associated vasculitis with tubulointerstitial nephritis was made. The 5 factors score proposed by French Vasculitis Study Group (2) that is predictive for prognosis in polyarteritis nodosa, microscopic polyangiitis and Churg-Strauss syndrome, showed 0, and the degree of vasculitis including mononeuritis multiplex and nephritis was relatively mild. Therefore, we started corticosteroid monotherapy with oral prednisone at 45 mg/day (1 mg/kg per day). She responded to this treatment with a normal ANCA titer and normal CRP level, resolution of proteinuria and of microhematuria, and an improvement in renal function. However, mild paresthesia persisted in the lower left leg. Prednisone dose was

tapered to 5 mg/day over 16 months, and serum creatinine level stabilized at approximately 1.0 mg/dL. ANCA remained negative.

## Discussion

Our patient was diagnosed with ANCA-associated vasculitis on the basis of her clinical symptoms, MPO-ANCA positivity and the pathological evidence of systemic vasculitis. The renal biopsy revealed focal crescentic necrotizing glomerulonephritis and diffuse tubulointerstitial nephritis extending in a vast area of the interstitium. The main pathophysiological problem is whether the diffuse tubulointerstitial nephritis is due to ANCA-associated vasculitis.

One possibility is that the diffuse tubulointerstitial nephritis might have been drug-induced. There have been several reports regarding MPO-ANCA–positive tubulointerstitial nephritis possibly due to medications such as indomethacin (3), ciprofloxacin (4), omeprazole (5) and cimetidine (6). Our patient had been given intravenous antibiotics and also NSAIDs before her first hospitalization. However, renal histology showed the acute or subacute phase of severe interstitial nephritis despite the discontinuation of these drugs long before the biopsy was performed. In addition, the infiltrated cells in the interstitium were mainly plasmacytes and neutrophils, not predominantly lymphocytes. Therefore, drug-induced tubulointerstitial nephritis was unlikely.

We also considered Churg-Strauss syndrome, because the patient had mononeuritis multiplex, mild peripheral blood eosinophilia and a history of allergies, but there were only a few eosinophils that had infiltrated the interstitium in the renal biopsy specimen, and the serum IgE level was within the normal range. Therefore, tubulointerstitial nephritis due to Churg-Strauss syndrome was also unlikely.

The renal pathological findings in ANCA-associated vasculitis are pauci-immune crescentic and/or necrotizing glomerulonephritis (7). Several studies have shown that 80%-90% of patients with ANCA-associated vasculitis have crescentic and/or necrotizing glomerulonephritis (7-10). On the other hand, tubulointerstitial injury in ANCA-associated vasculitis is generally thought to be secondary to crescentic glomerulonephritis, arteritis or arteriolitis (7). In a recent report, Sato et al suggested that peritubular capillary injury is the pathogenesis of tubulointerstitial changes in ANCA-associated vasculitis (11). Peritubular capillary injury – that is, peritubular capillaritis – has been highlighted in renal allograft nephropathy and results in interstitial fibrosis (12). The pathological findings of this patient showing diffuse and extensive tubulointerstitial changes may be compatible with peritubular capillaritis due to ANCA-associated vasculitis.

Tubulointerstitial damage rather than glomerular changes represents the major cause of renal dysfunction (10). Particularly, ischemia in the tubulointerstitium due to peritubular capillaritis leads to progressive renal failure (12). Therefore, it is important to pay attention to the degree of tubulointerstitial injury. Further studies are necessary to confirm the relationship between diffuse tubulointerstitial nephritis and ANCA-associated vasculitis.

Financial support: No financial support.

Conflict of interest statement: None declared.

*Address for correspondence:*
Hiroko Kanda, MD, PhD
Department of Allergy and Rheumatology
University of Tokyo
7-3-1 Hongo, Bunkyo-ku
Tokyo 113-8655, Japan
hkanda-tky@umin.ac.jp

## References

1. Banerjee A, McKane W, Thiru S, Farrington K. Wegener's granulomatosis presenting as acute suppurative interstitial nephritis. J Clin Pathol. 2001;54:787-789.
2. Bourqarit A, Le Toumelin P, Paqnoux C, et al; French Vasculitis Study Group. Deaths occurring during the first year after treatment onset for polyarteritis nodosa, microscopic polyangiitis, and Churg-Strauss syndrome: a retrospective analysis of causes and factors predictive of mortality based on 595 patients. Medicine (Baltimore). 2005;84:323-330.
3. Sakai N, Wada T, Shimizu M, et al. Tubulointerstitial nephritis with anti-neutrophil cytoplasmic antibody following indomethacin treatment. Nephrol Dial Transplant. 1999;14:2774.
4. Shih DJ, Korbet SM, Rydel JJ, Schwartz MM. Renal vasculitis associated with ciprofloxacin. Am J Kidney Dis. 1995;26:516-519.
5. Singer S, Parry RG, Deodhar HA, Barnes JN. Acute interstitial nephritis, omeprazole and antineutrophil cytoplasmic anti-

bodies. Clin Nephrol. 1994;42:280.
6. Kitahara T, Hiromura K, Sugawara M, et al. A case of cimetidine-induced acute tubulointerstitial nephritis associated with antineutrophil cytoplasmic antibody. Am J Kidney Dis. 1999;33:E7.
7. Jennette JC, Olson JL, Schwartz MM, Silva FG. Crescentic glomerulonephritis. In Heptinstall's Pathology of the Kidney. 5th ed. Philadelphia, PA: Lippincott Williams & Wilkins; 1998: 646-651.
8. Hauer HA, Bajema IM, van Houwelingen HC, et al; European Vasculitis Study Group (EUVAS). Renal histology in ANCA-associated vasculitis: differences between diagnostic and serologic subgroups. Kidney Int. 2002; 61:80-89.
9. Falk RJ, Nachman PH, Hogan SL, Jennette JC. ANCA glomerulonephritis and vasculitis: a Chapel Hill perspective. Semin Nephrol. 2000;20:233-243.
10. Samarkos M, Loizou S, Vaiopoulos G, Davies KA. The clinical spectrum of primary renal vasculitis. Semin Arthritis Rheum. 2005;35:95-101.
11. Sato S, Kitamura H, Adachi A, et al. Reduplicated basal lamina of the peritubular capillaries in renal biopsy specimens. J Submicrosc Cytol Pathol. 2005;37:305-311.
12. Aita K, Yamaguchi Y, Horita S, et al. Peritubular capillaritis in early renal allograft is associated with the development of chronic rejection and chronic allograft nephropathy. Clin Transplant. 2005;19 (Suppl 14):20-26.

*Received: January 19, 2008*
*Revised: March 04, 2008*
*Accepted: July 16, 2008*

Acta Neurol Scand 2010: 121: 127–130 DOI: 10.1111/j.1600-0404.2009.01272.x



ACTA NEUROLOGICA
SCANDINAVICA

## Clinical Commentary

# Less protease-resistant PrP in a patient with sporadic CJD treated with intraventricular pentosan polysulphate

Terada T, Tsuboi Y, Obi T, Doh-ura K, Murayama S, Kitamoto T, Yamada T, Mizoguchi K. Less protease-resistant PrP in a patient with sporadic CJD treated with intraventricular pentosan polysulphate. Acta Neurol Scand: 2010: 121: 127–130.


Treatment with intraventricular pentosan polysulphate (PPS) might be beneficial in patients with Creutzfeldt–Jakob disease. We report a 68-year-old woman with sporadic Creutzfeldt–Jakob disease who received continuous intraventricular PPS infusion (1–120 μg/kg/day) for 17 months starting 10 months after the onset of clinical symptoms. Treatment with PPS was well tolerated but was associated with a minor, transient intraventricular hemorrhage and a non-progressive collection of subdural fluid. The patient's overall survival time was well above the mean time expected for the illness but still within the normal range. Post-mortem examination revealed that the level of abnormal protease-resistant prion protein in the brain was markedly decreased compared with levels in brains without PPS treatment. These findings suggest that intraventricular PPS infusion might modify the accumulation of abnormal prion proteins in the brains of patients with sporadic Creutzfeldt–Jakob disease.

**T. Terada[1], Y. Tsuboi[2], T. Obi[1], K. Doh-ura[3], S. Murayama[4], T. Kitamoto[5], T. Yamada[2], K. Mizoguchi[1]**

[1]Department of Neurology, Shizuoka Institute of Epilepsy and Neurological Disorders, Shizuoka, Japan; [2]Department of Neurology, Fukuoka University School of Medicine, Fukuoka, Japan; [3]Division of Prion Biology, Department of Prion Research, Tohoku University Graduate School of Medicine, Sendai, Japan; [4]Department of Neuropathology, Tokyo Metropolitan Institute of Gerontology, Tokyo, Japan; [5]Department of Neurological Science, Tohoku University Graduate School of Medicine, Sendai, Japan

Key words: Creutzfeldt–Jakob disease, intraventricular infusion; pentosan polysulphate, prion protein

Tomokazu Obi, Department of Neurology, Shizuoka Institute of Epilepsy and Neurological Disorders, Urushiyama 886, Aoi-ku, Shizuoka 420-8688, Japan
Tel.: +81 54 245 5446
Fax: +81 54 247 9781
e-mail: obit@szec.hosp.go.jp

Accepted for publication September 3, 2009

### Introduction

Current options for the treatment of Creutzfeldt–Jakob disease (CJD) do not slow or halt disease progression. Treatment with pentosan polysulphate (PPS), a large polyglycoside molecule with anti-thrombotic and anti-inflammatory properties, administered intraventricularly to bypass the blood brain barrier can both prolong the survival period and reduce the extent of abnormal prion protein (PrP) deposition in the brains of rodent prion disease models (1). The safety and efficacy of intraventricular PPS treatment in humans with CJD, however, remains largely unknown (2–6). We report a patient with sporadic CJD (sCJD) treated with continuous intraventricular PPS administration starting 10 months after the onset of clinical symptoms.

### Case report

The patient was a 68-year-old woman with neither a family history of prion disease nor previous history of neurological disease. She had never received cadaveric growth hormone injection, a dura mater transplant, or a cornea transplant. She noticed unsteadiness of gait and forgetfulness at the age of 65 years. One month later, unsteadiness and intellectual deterioration progressed and myoclonic jerks appeared. Cerebrospinal fluid analysis was normal except for an increased concentration of neuron-specific enolase (66 ng/ml, normal < 25) and the presence of 14-3-3 protein. EEGs showed periodic spike/slow-wave complexes (spike-wave complexes). Diffusion-weighted MRI showed abnormal high-intensity signals in the head of the caudate nucleus, putamen and insular cortex.

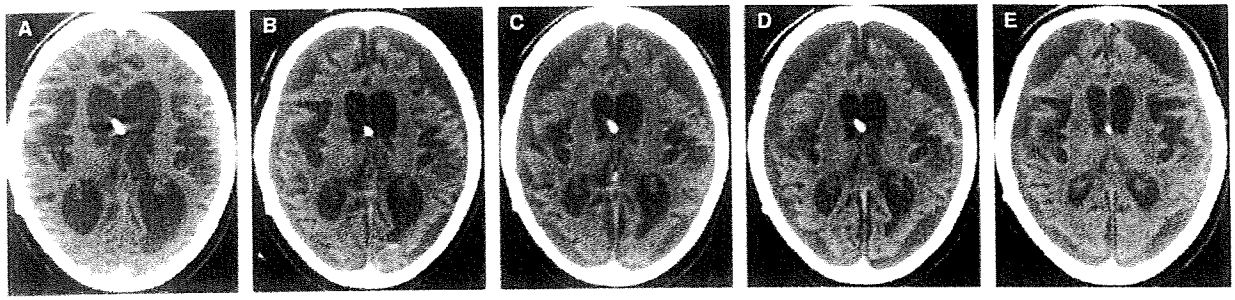


**Figure 1.** Sequential follow-up CT scans from 12 to 17 months after start of intraventricular PPS infusion. (A) Non-enhanced CT scan 12 months after start of intraventricular PPS infusion. Note the severe cortical and subcortical atrophy with enlargement of ventricular system. (B) Non-enhanced CT scan 13 months after start of intraventricular PPS infusion. Note the subdural fluid collection and the small sedimentation of blood in the left posterior horn. (C, D, E) Non-enhanced CT scan 14, 15, 17 months after start of intraventricular PPS infusion, respectively. The blood sedimentation in the posterior horn disappeared next month and subdural fluid collections were not progressing. No intraventricular hemorrhage was noted in scan E which was taken 7 days before death.

Genetic analysis of the *PrP* gene revealed methionine homozygosity at codon 129 and no mutations. The patient continued to deteriorate and became doubly incontinent, bed-bound and mute. Five months after the onset of symptoms, she developed akinetic mutism. Seven months after onset, the myoclonic jerks and spike-wave complexes disappeared. Ten months after onset, treatment with intraventricular PPS administration commenced under signed informed consent from her family. She received implantation of a right ventricular catheter and an epigastric subcutaneous drug infusion pump (Archimedes; 20-ml reservoir, flow rate 0.5 ml/24 h; Codman & Shurtleff Inc, Raynham, MA, USA). Using a reported protocol (5), infusion of intraventricular PPS (SP 54; bene-Arzneimittel GmbH, Munich, Germany) was started at 1 μg/kg/day, with subsequent escalation to the dose of 60 μg/kg/day 7 months later, and to the target dose of 120 μg/kg/day 15 months later, which continued until she died. However, her clinical condition did not improve and she still displayed akinetic mutism. A series of brain CT examinations demonstrated progressive brain atrophy, a transient intraventricular minor hemorrhage at the time of 13 months later, and a non-progressive collection of subdural fluid until 7 days before death (Fig. 1). Her clinical condition did not deteriorate from the time of 12 to 16 months. Monthly blood cell counts and coagulation measurements were normal. Twenty-seven months after onset, at age 68 years, the patient died of pneumonia which occurred 11 days before death and was aggravated.

## Methods

Autopsy was performed within 2 h after death. The right temporal pole of the brain was dissected out and stored at −70°C. The other parts of the brain were fixed in neutral buffered formalin. Sections of representative areas of the brain were stained with hematoxylin–eosin, Klüver–Barrera and immunohistochemical methods.

### Immunohistochemical staining

The following primary antibodies were used: anti-phosphorylated α-synuclein (monoclonal; Wako, Osaka, Japan), anti-phosphorylated tau (AT8, monoclonal; Fitzgerald, Concord, MA, USA), anti-amyloid β 1–42 (polyclonal; IBL, Takasaki, Japan) and anti-PrP (3F4, monoclonal; Signet, Dedham, MA, USA).

### Prion protein analysis

Protease-resistant PrP was extracted from cerebral tissues of this and other sCJD patients as previously described (7). Samples were subjected to 13.5% SDS-PAGE and transferred to polyvinylidene fluoride membrane. 3F4 antibody was used as the primary antibody. Anti-mouse EnVision (Dako, Glostrup, Denmark) was used as the secondary antibody. Enhanced chemiluminescence detection (Amersham Bioscience, Little Chalfont, UK) was used to visualize Western blots. The signal intensities of the blots were quantified with Quantity One software using an imaging device, Vasa Doc 5000 (Bio-Rad Laboratories, Hercules, CA, USA) (7).

For quantitative comparison of protease-resistant PrP levels, we initially analyzed 10-fold diluted samples derived from 0.5 mg wet-weight brain tissue from the temporal pole to identify suitable dilutions. For controls, we included frontal lobe tissues from three sCJD patients (all homozygous for methionine at codon 129 of the *PrP* gene) not treated with intraventricular PPS infusion: two with a type 1 pattern of protease-resistant PrP signals in Western blot analysis (sCJD MM1) whose brains were uniformly, severely atrophied similarly to the

patient's brain, and one with cortical-type sCJD and a type 2 pattern (sCJD MM2C).

## Results

### Post-mortem neuropathology

The unfixed brain weighed 660 g and showed walnut-shaped severe atrophy. A massive intraventricular hematoma was present. The shape of blood cells in the hematoma was completely preserved, with no infiltration by reactive cells such as macrophages and glial cells. The PPS infusion catheter had been correctly inserted into the right lateral ventricle, and the source of hemorrhage could not be identified. There was extensive, symmetrical cortical atrophy, but the hippocampi were relatively spared.

Microscopy demonstrated extensive neuronal loss and spongiosis in most areas of the cerebral cortices, with collapsed cytoarchitecture. Axonal loss with secondary myelin loss was present in the central white matter, accompanied by a cellular reaction containing both astrocytes and microglial cells throughout the areas of myelin damage. There was widespread gliosis in the basal ganglia, thalami and cerebellar molecular layer. The cerebellar granular layer showed marked neuronal loss with gliosis and axonal loss, accompanied by secondary myelin loss in the cerebellar white matter. Lewy bodies, amyloid plaques and neurofibrillary tangles were not observed. PrP staining showed a widespread synaptic pattern in the cerebral cortices, basal ganglia and thalami. Synaptic staining was also present in the molecular layer of the cerebellum, with intense coarse deposits in the granular layer. No plaque-like PrP deposits were identified in any brain regions. The findings were consistent with the diagnosis of sCJD. There was no laterality in the extent of the neuronal loss, spongiosis, gliosis or synaptic PrP deposition.

### Prion protein analysis

Western blot analysis of protease-resistant PrP showed a type 1 pattern (Fig. 2) identical to those of the two classical sCJD MM1 cases. Protease-resistant PrP levels were 1/3 to 1/8 of those in the sCJD patients with no intraventricular PPS treatment.

## Discussion

Here, we present a patient with sCJD who was treated with intraventricular PPS for 17 months. The PPS dose of 120 μg/kg/day was well tolerated

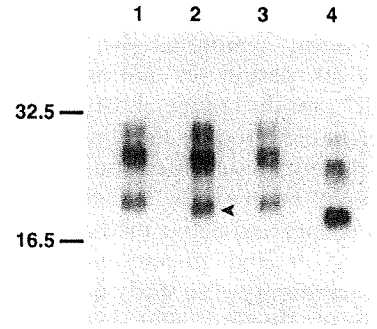


**Figure 2.** Comparative Western blot analysis of protease-resistant PrP. Protease-resistant PrP is categorized into three types based on the pattern of glycoform and mobility of PrP bands in Western blot analysis. Protease-resistant PrP, type 1, from the brain of this patient (threefold-diluted, lane 2) and three control subjects with sCJD: lane 1, 30-fold-diluted brain sample from an sCJD MM1 subject (65-year-old woman with a survival time of 11 months); lane 3, 20-fold-diluted brain sample from another sCJD MM1 subject (74-year-old woman with a survival time of 16 months); and lane 4, 40-fold-diluted brain sample from an sCJD MM2C subject. An unglycosylated PrP band from this patient (lane 2, arrowhead) mapped slightly lower than those in the other sCJD MM1 subjects (lanes 1 and 3). We normalized signal intensity to the band in lane 2 (100/mm$^2$). After dilution powers were also considered, the corrected signal intensities for lanes 1, 3 and 4 were 680/mm$^2$, 300/mm$^2$ and 770/mm$^2$, respectively.

but was associated with a minor, transient intraventricular hemorrhage and collection of subdural fluid. A fresh intraventricular hematoma found during autopsy probably occurred at the agonal stage, because blood cell shape was preserved and there was no inflammatory cell infiltration. Moreover, this intraventricular hematoma is unlikely to alter the patient's clinical course, because pneumonia which occurred 11 days before death was rapidly aggravated to respiratory failure responsible for her death, and no intraventricular hemorrhage was detected on CT scan 7 days before death.

Pentosan polysulphate is a candidate anti-prion compound that has shown efficacy in animal models (1, 8, 9), and has been administered by intraventricular infusion in several patients (2–6). Thrombocytopenia and abnormal coagulation can occur occasionally with PPS but did not occur in our patient. A minor, transient intraventricular hemorrhage and a non-progressive collection of subdural fluid appeared during PPS treatment but did not influence clinical progression. These findings may have resulted from a pressure imbalance within the intraventricular or subdural spaces caused by PPS infusion, although this speculation requires further proof. Overall, a PPS dose of 120 μg/kg/day seems well-tolerated and does not cause major adverse effects in CJD patients (2–6).

This patient survived for 27 months after the onset of clinical symptoms, which exceeds the mean survival period in national surveillance studies (12.7 months; range, 1–61) in Japan (10). PPS treatment did not alter the clinical course from the initial akinetic mute state. Thus, her prolonged survival might be partially attributable to both good nursing care and active medical interventions for malnutrition and pneumonia. The present study is a preliminary case study in a sCJD patient with pentosan therapy, and placebo-controlled study with PPS infusion will be needed in the future.

Prion protein deposition was not dramatically different between the hemisphere implanted with the catheter and the opposite hemisphere, unlike data reported in a rodent model (1). Here, the treatment started at an advanced clinical stage that may have already involved extensive PrP deposition, whereas treatment in the rodent model started before PrP deposition. In addition, difference of cerebrospinal fluid flow dynamics in the brain ventricular system between rodents and humans might contribute to the discrepancy. However, we found lower levels of abnormal protease-resistant PrP here than in other untreated sCJD patients, suggesting that PPS infusion might suppress the accumulation of abnormal PrP in the brain.

This speculation requires to be further evaluated, because there are possibilities that the gap of abnormal PrP levels between the patient and the control subjects might be attributable to the difference in disease durations or brain sampling regions, or to the regional variety of abnormal PrP deposition. These possibilities could not be evaluated in the present study because of limited sample availability.

**Acknowledgements**

The intraventricular PPS trial in this case was supported by a grant from the Japanese Ministry of Health, Labor and Welfare (H19-nanji-ippan-006).

**References**

1. Doh-ura K, Ishikawa K, Murakami-Kubo I et al. Treatment of transmissible spongiform encephalopathy by intraventricular drug infusion of animal models. J Virol 2004;**78**: 4999–5006.
2. Parry A, Baker I, Stacey R, Wimalaratna S. Long term survival in a patient with variant Creutzfeldt–Jakob disease treated with intraventricular pentosan polysulphate. J. Neurol Neurosurg Psychiat 2007;**78**:733–4.
3. Todd NV, Morrow J, Doh-ura K et al. Cerebroventricular infusion of pentosan polysulphate in human variant Creutzfeldt–Jakob disease. J Infect 2005;**50**:394–6.
4. Whittle IR, Knight RSG, Will RG. Unsuccessful intraventricular pentosan polysulphate treatment of variant Creutzfeldt–Jakob disease. Acta Neurochir (Wien) 2006;**148**: 677–9.
5. Rainov NG, Tsuboi Y, Krolak-Salmon P, Vighetto A, Doh-Ura K. Experimental treatments for human transmissible spongiform encephalopathies: is there a role for pentosan polysulfate? Expert Opin Biol Ther 2007;**7**:713–26.
6. Bone I, Belton L, Walker AS, Darbyshire J. Intraventricular pentosan polysulphate in human prion diseases: an observational study in the UK. Eur J Neurol 2008;**15**: 458–64.
7. Hizume M, Kobayashi A, Teruya K et al. Human Prion Protein (PrP) 219K is converted to PrPSc but shows heterozygous inhibition in variant Creutzfeldt–Jakob disease infection. J Biol Chem 2009;**284**:3603–9.
8. Farquhar C, Dickinson A, Bruce M. Prophylactic potential of pentosan polysulphate in transmissible spongiform encephalopathies. Lancet 1999;**353**:117.
9. Ladogana A, Casaccia P, Ingrosso L et al. Sulphate polyanions prolong the incubation period of scrapie-infected hamsters. J Gen Virol 1992;**73**:661–5.
10. Mizusawa H. Prion disease – an overview. Neurol Med 2005;**63**:409–16.

Case Report

European Neurology

Eur Neurol 2009;61:50–51
DOI: 10.1159/000175122

Received: December 19, 2007
Accepted: April 7, 2008
Published online: November 25, 2008

# Anti-N-Methyl-D-Aspartate Receptor-Related Grave but Reversible Encephalitis with Ovarian Teratoma in 2 Japanese Women Presenting with Excellent Recovery without Tumor Resection

Akihiro Shindo Ken Kagawa Yuichiro Ii Ryogen Sasaki Yasumasa Kokubo Shigeki Kuzuhara

Department of Neurology, Mie University Graduate School of Medicine, Mie, Japan

Acute encephalitis associated with ovarian teratoma preferentially affects young women and is characterized by acute prominent psychiatric symptoms, decreased level of consciousness, frequent seizures and central hypoventilation [1, 2]. Cases of reversible encephalitis affecting exclusively young women were reported in Japan under the name of 'acute juvenile female non-herpetic encephalitis (AJFNHE)' [3–5]. Dalmau et al. [6] recently reported that anti-N-methyl-D-aspartate receptor (NMDAR) antibody was positive in patients with acute encephalitis associated with ovarian teratoma as well as in mediastinum and grouped them in a category of NMDAR-related encephalitis. They recommended resection of the tumor for treatment [6–8], but it is not always easy for young nulligravid women to have their ovaries removed. We report NMDAR-related encephalitis in 2 patients treated without tumor resection.

### Patient 1

A 28-year-old woman developed curious behavior after persistent fever for 7 days, and suddenly became convulsive. On admission, consciousness was disturbed and temperature was high. General physical examination revealed neck stiffness and Kerning sign. Blood cell counts and routine serum biochemical analyses were normal. Serological testing for antinuclear and anti-DNA antibodies, tumor markers and syphilis were negative. Her cerebrospinal fluid (CSF) showed mild pleocytosis, was negative for tubercle bacilli on culture and for herpes simplex virus (HSV)-DNA on PCR. Brain MRI showed no abnormalities. The pelvic CT showed bilateral ovarian teratoma. EEG showed diffuse delta waves with no epileptic discharges. Intravenous administration of acyclovir was continued until the result of HSV-DNA on PCR was confirmed. Administration of methylprednisolone and antiepileptic drugs was started. However, her condition worsened gradually, and she presented with stereotypic oral dyskinetic movements. She fell in hypoventilation and coma, and was put on a ventilator. Her condition began to improve and ventilatory support was withdrawn on the 50th hospital day. She was discharged 83 days after hospitalization with excellent recovery.

Antibodies to NR1/NR2B heteromers of NMDAR in the serum and CSF were positive on admission. One year after, the serum NMDAR antibodies were no longer detected. The pelvic MRI showed bilateral ovarian teratomas (fig. 1A), and the tumors did not change in size for 1 year.

### Patient 2

A 33-year-old woman developed persistent fever and cried violently. High fever continued and seizure-like involuntary movements occurred. General physical and neurological examination showed neck stiffness and bilateral positive Babinski sign. The CSF showed mild pleocytosis, The pelvic CT revealed right ovarian teratoma. She received anticonvulsant medications and methylprednisolone pulse therapy. Because of hypoventilation, she was put on mechanical ventilation for 10 months. Her condition began to improve, and she was transferred for rehabilitation. Neurological examination 4 years after onset revealed excellent recovery.

The NMDAR antibodies in the CSF at the acute stage were positive. Serum NMDAR antibodies were not detected 5 years after discharge. Pelvic MRI showed right ovarian teratoma (fig. 1B), and the tumors did not change in size for 5 years.

### Discussion

As to the treatment of NMDAR-related encephalitis, tumor resection was recommended [6–8], since patients with tumor resection had recovered while those without resection worsened or died [6]. In con-

KARGER

Fax +41 61 306 12 34
E-Mail karger@karger.ch
www.karger.com


0014–3022/09/0611–0050$26.00/0

Accessible online at:
www.karger.com/ene

Akihiro Shindo, MD
Department of Neurology, Mie University Graduate School of Medicine
2-174 Edobashi, Tsu
Mie 514-8507 (Japan)
Tel. +81 59 232 1111, Fax +81 59 231 5082, E-Mail a-shindo@clin.medic.mie-u.ac.jp